The post-Variscan tectonic-thermal activity in the southeastern metalliferous province of the French Massif Central revisited with K-Ar ages of illite

Norbert Clauer

The post-Variscan tectonic-thermal activity in the southeastern metalliferous province of the French Massif Central revisited with K-Ar ages of illite

Norbert Clauer

Institut de Physique du Globe de Strasbourg, (CNRS-UdS), Université de Strasbourg, 1, rue Blesssig, 67084 Strasbourg, France

corresponding author: Dr. Norbert Clauer, Institut de Physique du Globe de Strasbourg (CNRS-UdS), Université de Strasbourg, 1 rue Blessig, 67084 Strasbourg, France, e-mail: nclauer@unistra.fr

Keywords: illite-type clays, southeastern French Massif Central, K-Ar dating, Pb-Zn metal district

Abstract

This study deals with K-Ar data of illite and illite-rich mixed-layers of Cambrian and Permian metasediments that were subjected to tectono-thermal episodes in the Montdardier and Mas Lavayre ore districts of the southeastern Massif Central (France). The objective was to differentiate events that altered the metal-rich deposits from those that affected only barren host rocks close to the ores. On the basis of combined mineralogical analyses and isotopic determinations of the clay material, successive tectono-thermal events induced illitization at 288 ± 10, 246 ± 9, 197 ± 6, 176 ± 6 and 107 ± 4 Ma and probably at 136 ± 4 Ma.

The lack of major geodynamic activities near the studied ore deposits during these times hypothesizes periodic long-distance migrations of fluids in the continental crust to explain their occurrences. Metals seem to have been concentrated at specific places, but apparently they were not deposited or altered during post-Visean tectono-thermal pulses recorded by the associated illite. The tectonic-thermal history of the Les Malines district confirms that repetitive geodynamic re-activations induced local heat transfers. However, the episode at 246 $\pm$ 9 Ma apparently did not affect the earlier deposited ores, while that at 35-40 Ma found in coffinite at Pierre Plantées was probably not induced by a thermal event, but by an alteration event that did not affect the K-Ar system of the surrounding clay material.

Introduction

Isotopic dating represents a valuable contribution to reconstruct the genetic evolution of sediment-hosted ore deposits. However, the gained information is not straightforward, as the recent analytical/technical improvements have not solved all uncertainties in ore isotopic dating. For instance, among the identified difficulties is the lack of the precise knowledge of the initial Pb isotopic compositions of metals (Romer, 2001), or the tendency of ores to easily recrystallize when environmental conditions change, which potentially can modify their chemical and isotopic compositions of the U-Pb system. Also, uranium minerals often contain large amounts of radiogenic Pb that allow a routine application of the U-Pb dating method; but their timing of crystallization is sometimes questionable because intermediate isotopes from uranium decay chain may escape from the host minerals exposed to subsurface conditions (e.g., Miller and Kulp, 1963; Holliger et al., 1989).

Due to these inherent difficulties, indirect isotopic dating of ore deposits has been explored in recent decades as a complementary approach to direct isotopic dating. This indirect dating consists of the study of barren minerals associated with the ore concentrations that record the same evolution (e.g., Clauer and Chaudhuri, 1992). Among barren minerals often associated with ore deposits in sediments and metasediments are clay minerals that can be considered potential age markers using basic isotopic methods (e.g., Ineson et al., 1975; Halliday and Mitchell, 1983). In fact, the information from such studies of barren minerals

61 can be extended beyond strict age comparison by evaluating the physical-chemical parameters
62 that control the evolution of an entire ore district. Clay minerals have the advantage, which
63 can sometimes also be a drawback, to be sensitive to discrete changes in the chemical and/or
64 thermal conditions of a complex regional tectonic-thermal evolution (e.g., Clauer and
65 Chaudhuri, 1995). Easily identified by appropriate methods including X-ray diffraction and
66 electron microscopy, their study also has some inconveniences as it is sometimes difficult to
67 separate authigenic from detrital clay crystals even by sophisticated separation methods. In
68 fact, many studies of clay minerals from uranium deposits benefitted by such combined
69 geochronological approaches (e.g., Lee and Brookins, 1978; Bell, 1985; Clauer et al., 1985;
70 Bray et al., 1987; Brockamp et al., 1987; Turpin et al., 1991). Studies on stable and
71 radioactive isotope compositions of clay minerals from uranium deposits have also
72 highlighted how thermal and chemical information registered by such barren minerals can
73 support and even improve our understanding of ore deposits (e.g., Halter et al., 1987; Wilson
74 et al., 1987; Kotzer and Kyser, 1995; Kyser et al., 2000; Polito et al., 2006; Laverret et al.,
75 2010). Since age discordances are often systematically reported in ore deposits and in
76 associated barren host rocks, a detailed examination of the genetic relationship of both types
77 of minerals appears justified and timely. In turn, the present study was designed to continue
78 decrypting the tectonic-thermal evolution of a large ore region to investigate if all events
79 recorded by the clay material from barren host rocks also occur in the ore deposits. The use of
80 clay minerals for geochronological information of ore deposits emphasizes the following
81 concern: since clay minerals potentially record any hydrothermal event (e.g., Velde, 1985),
82 how can one unequivocally identify those interacting with the metal deposits in an ore district
83 from those having no impact?
84 To identify the successive affects of such regional evolution on ore concentrations, the
85 present review provides a compilation of K-Ar data of illite separates of Cambrian and
86 Permian ore-hosting and barren rocks from southeastern French Massif Central. The attempt
87 here is to answer the question whether the known ore concentrates had or had not an
88 independent evolution relative to the surrounding regional host rocks.
89
90 ## Geological setting and sampling
91

In the southeastern French Massif Central, the Paleozoic basement hosts a major metalliferous province that produced about 2 million tons of Pb-Zn metals since the initiation of exploitation. Towards its northern area, the basement consists of late Variscan granites (Hamet and Mattauer, 1977; Vialette and Sabourdy, 1977), whereas the Causses-Shoal structural unit to the west and the south results from Triassic-to-Jurassic (Callovian) tectonic faulting, together with changes in the lithology and sedimentation rates of the cover sediments (e.g., Clauer et al., 1997). The whole district is located along the major Cévennes fault system, to the SE of the Massif, active as a normal fault, at least during the Liassic extensional period (Lemoine, 1984). The plutonic basement is overlain by Cambrian to Triassic dolomite-rich black shales and Bathonian dolostones followed by Oxfordian dolomite shales (Le Guen and Combes, 1988).

The genesis of the Pb-Zn and U deposits in this southeastern part of the Massif Central has been explained by various mineralizing processes, from a karstic (Orgeval, 1976; Connan and Orgeval, 1977; Verraes, 1983) to a syngenetic (Macquar, 1970; Michaud, 1970) and to a diagenetic type (Bernard, 1958; Fogliérini et al., 1980), as well as by interactions with migrating hydrothermal fluids (Charef and Sheppard, 1988; Ramboz, 1989; Le Guen et al., 1991), demonstrating in turn that there is no unanimity about their genesis. Based on Pb isotopes to trace and constrain the genesis of the Pb-Zn ores, Le Guen et al. (1991) considered that the Pb-Pb isotopic compositions of the different ore bodies were quite homogeneous, ruling out a major contribution of external Pb during the successive concentration/remobilization episodes. In fact, such a model confirms the hypothesis of an initial stock of Pb that evolved continuously in an almost closed system at a regional scale, without any significant supply of external Pb or loss of initial Pb.

Lancelot et al. (1995) reviewed the U-Pb and Pb-Pb data of three major regional U deposits: those of the southeastern Lodève and of the central Bertholène and Pierres Plantées. The results suggest a generalized precipitation of metallic ores during the Liassic (between 195 and 175 Ma), and a common multi-stage evolution. Despite the diversity of the host rocks, such as Permian sediments above the unconformity with the Variscan basement at Lodève, the orthogneissic and mylonitic Variscan basement at Bertholène, and the episyenitic veins cutting post-tectonic Variscan leucogranites at Pierres Plantées, the U-Pb and Pb-Pb data point to a major Liassic U concentration induced by fluid circulation at temperatures

123 from 140 to 250°C and salinities from 5 to 14% NaCl eq. At Pierres Plantées, a pre-
124 concentration was also identified at about 270 Ma in leucogranite veins percolated by fluids at
125 300-350°C. At Bertholène, the U contents were dated at about 170 Ma as tiny spherules
126 disseminated in altered Oligocene coffinite. Further U remobilization was detected at Lodève
127 and Pierres Plantées during the Cretaceous, which was confirmed in the southeastern deposits
128 by K-Ar dating of clays from gouges of the Saint-Julien fault that contain U minerals
129 (Mendez Santizo et al., 1991).

130 Analyzed earlier by Vella (1989) and Mendez Santizo (1990) in their PhDs, the K-Ar
131 data of varied illite-rich size fractions (<0.2, <0.4, 0.4-1, 0.4-2 and <2 μm), separated from 26
132 Paleozoic samples from two southeastern locations from French Massif Central are combined
133 and re-examined here (Fig. 1A to D; Table 1). In the northern part of the selected area, six
134 Cambrian calcschists were collected in and next to the Montdardier mine about 3 km to the W
135 of the Les Malines district (Fig. 1C), together with two more argillaceous dolostones taken in
136 the neighborhood of the mine. In the second sector about 50 km to the SW, four Autunian
137 samples were collected in the Mas Lavayre mine with five samples from a transect across the
138 Saint-Julien fault visible in the mine at about 5 km to the SE of the Lodève district, and six
139 core splits of the exploration drilling MLV located 1 km to the E of the Mas Lavayre mine
140 (Fig. 1D). In addition to these clay-rich samples, five feldspar separates purified from
141 interlayered pyroclastic to tuffaceous beds of Autunian sediments from Mas Lavayre mine
142 were also purified, analyzed for their K-Ar data and the results are included into the
143 discussion.
144
145 **Analytical procedure**
146
147 As the rock samples were quite indurated, gentle freeze-thaw disaggregation
148 consisting of repetitive cycles of freezing at -25°C and heating at +25°C applied to 1cm^3 rock
149 chips sealed in polyethylene bottles filled with de-ionized water (Liewig et al., 1987) proved
150 to be insufficient. This method was replaced by hand crushing of whole-rock chips in an agate
151 bowl and separating the <2 μm size fractions from rock powders by dispersion and
152 sedimentation in de-ionized water and recovery by applying Stoke's law. The complementary
153 size fractionations (<0.2, <0.4, 0.4-1 and 0.4-2 μm) were completed on the extracted <2 μm

fractions by ultracentrifugation. The size fractions were X-rayed (XRD) with determination of the illite crystallinity index (ICI) of the (001) illite peak following Kübler's (1968; 1997) concept and called now full width at medium height (FWMH). Theoretically, the FWMH (ICI) values below 0.25 define epizonal metamorphic conditions, those between 0.25 and 0.37 define anchizonal metamorphic conditions and the higher values correspond to a diagenetic grade. The limits depend on the analytical conditions and the characteristics of the used XRD equipment (here operated at 40 KV/20 mA and equipped with a Cu anticathode and a Ni filter and slits of 1 and 2° for the tube and the counter, respectively). Special attention was given to identify the potential detrital minerals in the separated size fractions, such as micas and feldspars, as they potentially bias the isotopic ages of the authigenic minerals. The feldspar separates were purified by disaggregating the tuffaceous samples with the above freeze-thaw technique, sizing the slurries by wet-sewing, and purifying the fractions in dense liquids. The separated size fractions were X-rayed, which showed that they were almost never pure but always mixed with minute amounts of albite, quartz and muscovite. The two former minerals have no impact on the K-Ar data, the occurrence of the latter is of some concern, so that only the size fractions without any muscovite peak in the XRD patterns were analyzed.

The K-Ar determinations were obtained following the procedure of Bonhomme et al. (1975) that has been described in varied publications of the group. The powders of the different size fractions were preheated at 100°C during 12 hours under vacuum in the extraction line to remove any atmospheric Ar adsorbed on the clay particles during sample preparation, handling and size separation. The accuracy of the Ar extraction method was periodically controlled by analysis of the international GL-O standard mineral with the radiogenic ^{40}Ar content averaging $24.54 \pm 0.15 \times 10^{-6}$ cm^3 (2σ) for 4 independent analyses during the course of the study. The $^{40}Ar/^{36}Ar$ ratio of the atmospheric argon was also periodically measured, giving an average of 295.0 ± 1.9 (2σ) for 5 independent analysis, also during the course of the study. Since the results were analytically consistent and close to the theoretical values of $24.85 \pm 0.24 \times 10^{-6}$ cm^3 ^{40}Ar for the GL-O standard (Odin et al., 1982), and 295.5 for the atmospheric $^{40}Ar/^{36}Ar$ ratio used at the time the samples were analyzed (Nier, 1950), no correction was applied to the raw data. As the sample analyses were quite ancient, the differences with the values of the standards had almost no impact on the final ages. The blank of the gas extraction line and its coupled mass-spectrometer was also checked

weekly before the Ar extraction. Systematically below 10^{-8} cm^3, the amounts of radiogenic ^{40}Ar of the blank were two orders of magnitude lower than the amounts of that extracted from samples and, therefore, they were considered not to bias the data. The K contents were determined by flame spectrometry and the K-Ar ages calculated with the usual decay constants (Steiger and Jäger, 1977). The final precision of the K-Ar ages was estimated to be better than 2%. To remind the readers, especially those unfamiliar with illite K-Ar isotope dating but having a preference for the application of the more recent "sister" $^{40}Ar/^{39}Ar$ dating technique of illite, the specific advantages and drawbacks of the two K-Ar and $^{40}Ar/^{39}Ar$ dating methods were evaluated and compared by a systematic application of both methods on the same illite-sized separates (Clauer et al., 2012; Clauer, 2013).

Results

The XRD results

The separated size fractions are quite similar on the basis of the XRD results. They consist mainly of illite mixed with illite-smectite mixed layers (labeled I-S hereafter) in five Permian samples of the Mas Lavayre mine and in the deepest sample of the MLV354 drilling, with chlorite (up to 80-90% in the four deeper Permian samples of the MLV354 drilling), or kaolinite (traces to 15% in three Montdardier fractions; Table 2). Most FWMH of the finest <0.4 μm fractions are below 0.36 (Table 2), while only the <0.4 μm fraction of the Montdardier M1 sample, of three samples from Mas Lavayre mine and of its associated MLV354 drilling yield higher values. Consequently, most illite fractions are within the epizonal (low-grade metamorphism) and the lower anchizonal domains, which suggests crystallization temperatures between 160 and 280°C (Kübler, 1997).

The three F1 feldspar separates contain pyrite, pyrolusite, quartz, and galena for the 80-100 μm fraction, quartz for the 125-200 μm fraction, and apatite, blende and quartz for the 200-400 μm fraction. The 125-200 μm fraction of the F2 feldspar contains pyrite, blende, quartz and pyrolusite.

The K-Ar data

215 At a first glance, the 43 K-Ar data range widely from 298.3 ± 13.7 to 103.0 ± 3.5 Ma
216 (2σ; Table 3). The K-Ar ages of the five complementary feldspar separates split into two
217 groups at 282 ± 13 Ma for three of them and at 255 ± 9 Ma for the two others. Among the
218 illite ages, 16 were measured on the finer <0.2 and <0.4 μm sub-fractions that were extracted
219 and analyzed separately to evaluate if the coarser <2 μm fractions are isotopically
220 homogeneous, or if they consist of several generations of illite-type particles characterized by
221 an increasing amount of younger generations in the finer fractions and of older generations in
222 the coarser fractions. In fact, 5 samples yielded K-Ar ages within analytical uncertainty for
223 their 2 analyzed size fractions. Those of the Cambrian LM1 argillaceous dolomite from Les
224 Malines mine yield an average age of 290 ± 8 Ma, and those of the MLV4 Permian sample of
225 the nearby drilling MLV354 provide an average age of 176 ± 7 Ma. In the case of the two SJ3
226 and SJ4 <0.2 and <0.4 μm fractions, the K-Ar values are also within analytical uncertainty at
227 136 ± 4 and at 107 ± 4 Ma, respectively. This preliminary check of the K-Ar results suggests
228 episodic illitization at about 290 Ma, 175 Ma, 135 Ma and 105 Ma. On the basis of these
229 results, it appears that the <2 μm size fractions with identical ages consist of homogeneous,
230 authigenic illite populations, as is the case for the samples M3, M4, M6, MLV6, and for the
231 feldspar separates F1a, F1b and F2. The K-Ar data of the 0.4-2 μm size fractions of the M5,
232 M6, ML1, ML2, SJ2, MLV4 samples also fit these preliminary age groupings, as well as that
233 of 0.4-1 μm size fraction of SJ3 sample. The 0.4-1, 0.4-2 and <2 μm fractions of the other
234 samples with older K-Ar data, therefore suggest that they consist of multi-generation material
235 including detrital components. In summary, it can be considered at this point that half of the
236 forty-eight available K-Ar data apparently identify four well-defined tectono-thermal
237 illitization episodes.
238 Harper (1970) plots compare basically the contents of the radiogenic ^{40}Ar relative to
239 those of the K of the illite and feldspar fractions. Here, four lines can be drawn through
240 several alignments of data points that end at the intersection of the coordinates as they should
241 (Fig. 2). These lines are not strictly isochrons, such as those of $^{40}Ar/^{36}Ar$ vs. $^{40}K/^{36}Ar$
242 correlations. However, average ages can be calculated by combining the individual ages of all
243 representative data points of each line. In the detail, the upper line with the steepest slope is
244 anchored by three feldspar and six illite data points at an average age of 288 ± 10 Ma. The
245 line below is less constrained with two feldspar and three illite data for an average age of 246

± 9 Ma. The next line below fits through six illite data points, giving an age of 197 ± 6 Ma. Finally, the line with the lowest slope includes seven data points of illite-rich fractions, giving an age of 176 ± 6 Ma. The leftover data points that are scattered in between the references lines, can be assumed to result from a mix of minerals crystallized during at least two of these episodes (Fig. 2). In summary, by combining the four K-Ar ages obtained from checking those of the different size fractions of the same samples and the four ages from lines in the radiogenic ^{40}Ar vs. K diagram, the ages at about 290 Ma and 175 Ma were found in both evaluations. The size fractions with the younger ages at about 135 and 105 Ma that were not obtained in the Harper (1970) plot also contain I-S mixed layers, suggesting some alteration of illite into K-depleted smectite. This could be due to a hydrothermal influence related to the motion of the Saint-Julien fault.

The coarser size fractions (0.4-1, 0.4-2 and <2 μm) of the Cambrian samples range either around 280-300 Ma or on the older side of the 180-200 Ma group, which confirms the timing of these episodes and shows also that the 220-260 Ma and the 150-100 Ma events apparently did not affect the Cambrian metasediments. Conversely, the older K-Ar data of the coarse Permian size fractions are obviously biased by detrital contaminants with K-Ar data either similar to the deposition age of the host rocks, or even older. Most of the other K-Ar data of the Permian material are on the older side of the 170-190 Ma event, which suggests some resetting (Table 3).

Discussion

The broadly range ofthe K-Ar ages suggest crystallization of several generations of illite during distinct thermal episodes in ore-bearing and barren Cambrian and Permian sediments of the southeastern mining district of the French Massif Central. This evolutionary sequence occurred along the eastern Cevennes fault system that acted as the regional circulation drain for advective fluids. Illite of the sampled rocks was altered either once or several times, completely or incompletely, or even not at all.

<u>The paleo-thermometric context</u>

A paleo-thermometric study showed that bi-phased aqueous inclusions of quartz from faults in the nearby Upper Permian yield homogenization temperatures from 60 to 300°C (Staffelbach et al., 1987; Mendez Santizo et al., 1991). In fact, most of the inclusions yield homogenization temperatures from 150 to 300°C with a maximum frequency at 170-180°C in the major fractures such as that of Saint-Julien sampled in the Mas Lavayre mine. Those above 240°C obtained on quartz inclusions correspond to fusion temperatures at salinities between 16.5 and 12% eq. NaCl. The fractionation coefficient of Co between pyrite and pyrrhotite being temperature dependent (Bezmen et al., 1975), two sets of temperatures were obtained for the pyrite-pyrrhotite association in the Saint-Julien fault: 280 $\pm$ 6°C for the gouge material, and 242 $\pm$ 22°C for vein deposits in the host rocks. This latter temperature does not match a diagenetic impact for the 250-Ma illite resulting from alteration of pyroclastic material (Brockamp and Clauer, 2013), unless the veins with pyrite-pyrrhotite infillings formed during moving of the Saint-Julien fault.

The obtained large temperature spectrum confirms that various thermal conditions necessarily occurred in rocks of different stratigraphic ages and locations, including the fact that the diagenetic/hydrothermal conditions must have happened soon after sediment deposition during the Permian. The 185 $\pm$ 11 Ma episode appears to have had a climax impact in various stratigraphic strata: in Permian sediments at Lodève, as well as in U-enriched veins nearby Rabejac (Lancelot and Vella, 1989). Such a paroxysmal activity was reported during the Rhaetian–Hettangian time in the Cévennes and western Alps, which corresponds in turn to the development of the Ligurian Tethys (Lemoine et al., 1986; Dromart et al., 1998). The 105 $\pm$ 5 Ma episode determined in gouge material of the Saint-Julien fault (Mendez Santizo et al., 1991) has also been considered to correspond to the onset of the first oceanic accretion in the Biscay Bay (Montadert et al., 1979).

The historical context of the ore genesis in the southeastern Massif Central

For Charef and Sheppard (1988), the main ore stage is characterized by the mixture of fluids with a metal-rich brine at a temperature of about 150°C that the authors identified as a connate water resulting from dewatering of the basin. Called the “Neo-Variscan stage” by Merignac and Cuney (1999), this episode of main metal concentration is characterized by a shift from a compressional to an extensional tectonic regime and a significant heat-flow

circulation. Conversely, Early-Jurassic illite ages discussed by Clauer and Chaudhuri (1995) as representative of tectono-thermal activities in the Les Malines sector were denied by Leach et al. (2001) who attributed them to a widespread diagenetic event in the host rocks. However, the alternative model of Leach et al. (2005) based on gravity-driven fluid movements for some of the known deposits is equally questionable. Indeed, it is because of the high temperatures determined in fluid inclusions from minerals associated with the ore deposits evaluated in the previous section, and because of the episodic K-Ar ages obtained here. Finally, after decades of varied models based on the re-activation of karst infillings, the metal deposits were also considered by the same authors to result from fluid migrations during a 60-Ma old compressional tectonic event on the basis of a well-defined remagnetization (Henry et al., 2001; Rouvier et al., 2001). They attributed this overprint to a chemical process due to a major uplift in the Pyrenean mountains with fluid migrations from south to north. However, on the basis of conclusions contradicting the earlier interpretations by Macquar et al. (1990) of a Triassic origin of the metal concentrations, the authors admitted a tectonic influence in the evolution of the ores from southeastern Massif Central. The 60-Ma age is, however, far too young relative to the neo-Visean concentrations and the illite K-Ar ages obtained here.

The published K-Ar ages of illite from metasediments of the Massif Central are somewhat of an "uneven" analytical level as many were obtained on <2 μm illite-rich size fractions (Bellon et al., 1974; Bonhomme and Millot, 1978; Bonhomme et al., 1983; Bril et al., 1991; Brockamp and Clauer, 2013). It has long been demonstrated that such coarse clay fractions often contain detrital minerals that bias the "ages" by increasing the data (Fig. 3). However, despite this technical aspect, the published ages are never strictly related to the major Variscan episodes. In other words, they are never older than 300 Ma and, therefore, the U-Pb and Pb-Pb ages of regional metal deposits of the Variscan period were discarded in this review. Post-Variscan U concentrations in the region seem to have begun about 270 Ma in leucogranite veins percolated by fluids at 300-350°C (Lancelot et al., 1995). Later concentrations were dated at 188 $\pm$ 12 Ma in a pitchblende (Respaut et al., 1991), at 172 $\pm$ 9 Ma in uraninite (Léveque et al., 1988), at about 100 Ma in a coffinite, and even at 35-40 Ma at Pierres Plantées, again in a coffinite (Respaut et al., 1991). This last age is the only one that occurred after the potential Pyrenean activity mentioned just above. Some U concentration was also detected at about 170 Ma in coffinite at Bertholène. All these recorded ages are far

from the Pyrenean activity detected in the southern Massif Central by remagnetization (Rouvier et al., 2001).

Meaning of the illite K-Ar ages from southeastern Massif Central

Alternatively to the single paleomagnetic record just mentioned, K-Ar illite ages were reported between 220 and 160 Ma in the Lodève area (Bellon et al., 1974; Bonhomme and Millot, 1978; Bonhomme et al, 1983). At the Bernardan site, six illite K-Ar ages average 161 ± 9 Ma (Clauer, unpublished) with four more values scattered between 240 and 185 Ma. Lancelot et al. (1994) detected also two U remobilizations by K-Ar dating of illite from Lodève district at 173 ± 6 and 108 ± 5 Ma. These authors connected the first of these two events to an extensive thermal event of the continental crust to the south of the Massif Central. Clauer et al. (1997) reported a K-Ar age of 190 ± 20 Ma for an illite infilling a major fault in the carbonate-rich, passive paleo-margin along the southeastern Massif Central.

It is generally agreed that age identities of two fine-size fractions from the same samples corroborate with geological meaningful ages, as discussed by Clauer and Chaudhuri (1998) who illustrated this behavior by a "bench-type" sketch with the same age having a geological meaning for the fine fractions, and an older meaningless date for the coarser fraction(s). If the fine (<0.2 or <0.4 μm) fractions consist mainly (or only) of authigenic illite and, depending on the deposition time of their host sediments, a multi-episodic tectonic-thermal activity can be postulated at 288 ± 10 Ma based on the K-Ar of the pyroclastic feldspars and of illite separates from sediments of Les Malines deposits, as well as at 246 ± 9 Ma mostly in the Cambrian sediments from the Les Malines district with a further late illite crystallization at 105 ± 5 Ma in gouge material of the Saint-Julien fault in the Mas Lavayre mine (Mendez Santizo, 1990; Mendez Santizo et al., 1991).

Brockamp and Clauer (2013) studied diagenetic and hydrothermal impacts and their timing in illite-rich size fractions of Permian shales close to the Lodève U-district located about 4 km to the NW of the northern sector studied here. There, illite with a mean K-Ar age of about 260 Ma is the predominant mineral in the shales. It is of early diagenetic origin relative to deposition and apparently formed directly from deposited pyroclastic materials, which waives the problem of a detrital contamination as such rock type basically does not contain detrital minerals. The associated hydrothermally altered shales next to the U-deposit

369 also contain a K-feldspar generation with K-Ar ages clustered around 220 Ma, although
370 Jurassic and Cretaceous ages were also obtained. The hydrothermal temperatures were
371 estimated to be below 200° C as the early diagenetic illite is only partially reset. It looks like
372 Triassic fluids ascended along faults into the northern part of the Lodève basin during an
373 initial rifting of the nearby western Tethys Ocean. Later fluid pulses were also recorded at
374 Lodève during the opening of the North Atlantic and separation of Europe from Africa
375 (Jurassic/Cretaceous). Along with this tectono-thermal activity, successive pulses of hot fluids
376 of crustal origin apparently also penetrated the Lodève district.
377 In summary, the early thermal event at 288 ± 10 Ma obtained in the pyroclastic
378 feldspars and in the Montdardier Cambrian sediments was expectedly not recorded in the
379 Permian sediments that were deposited later. The later 246 ± 9 Ma episode was also recorded
380 in Permian sediments at Mas Lavayre. By itself, evidence of a volcanic activity does not
381 necessarily imply regional abnormal thermal conditions in sediments: thermal conditions are
382 diffusing wider when detected in sediments of varied stratigraphic ages and from different
383 locations, which strengthens the argument for regional abnormal thermal conditions.
384
385 The regional extent of illite K-Ar ages relative to the evolution of the metallogenic deposits
386 The K-Ar data of the illite-type clay material studied here fit well into the late plutonic
387 and structural geologic framework of the post-Variscan plutonic history and the Liassic
388 extensional tectonic episode along the Cévennes fault system. The review by Lancelot et al.
389 (1995) summarizes the regional ore formation in which the ages obtained here fit well. The
390 same regional picture applies also to fault gouges filled with clay minerals in plutonic and
391 sedimentary rocks to the NW of the Massif Central (Cathelineau et al., 2004). There, the
392 finest <0.2 μm fractions from deep fractures (>570 m) yield older ages, from 272 to 253 Ma,
393 than those of 198 to 188 Ma for illite from shallow-depth fractures. This confirms the
394 occurrence of two distinct episodes, probably of different intensity. Cathelineau et al. (2012)
395 showed that migrating brines and seawater interacted with both the sedimentary cover and the
396 crystalline basement in the Poitou High at the northwestern edge of the French Massif
397 Central, from 156 to 146 Ma based on K-Ar dating of illite and $^{40}Ar/^{39}Ar$ dating of associated
398 feldspars. This hydrothermal activity induced significant dolomitization and silicification of

399 the sediments, adularization of the granitic basement, and local concentrations of F–Ba (Pb–
400 Zn) assemblages.
401 All these results confirm the occurrence of geographically dispersed and episodic
402 hydrothermal activities at different metalliferous sites. Illite crystallization often occurred in
403 nearby fault systems that acted as drains for migrating fluids that favored or not ore genesis.
404 As a possible alternative to this scenario, late-Variscan activities in plutonic basement rocks,
405 especially of the major cratonic basement of Western Europe, were not often reported.
406 In summary, the compilation of the illite K-Ar and ore U-Pb and Pb-Pb ages outline
407 several age combinations for the regional tectono-thermal activity (Fig. 3). After the Variscan
408 stage, a regional episode is detected by illite K-Ar ages from NW to SE of the Massif Central
409 at 305-285 Ma. A following event was also widely detected from NW to SE at 265-245 Ma.
410 The next episode occurred at 210-190 from NW to SE immediately followed by another in the
411 NW and the SE areas at 185-160 Ma, assuming these events were not connected. The two last
412 episodes are less spread out, one to the N at 150-135 Ma and the last to the S at 120-105 Ma.
413 Only the later of these episodes affected the ore deposits: that at 210-190 Ma at Pierres
414 Plantées and Rabejac, that at 185-160 Ma again at Pierres Plantées and at Lodève and the final
415 episode at 120-105 Ma at Lodève.
416
417 Combining U-Pb and Pb-Pb dating of ores with K-Ar dating of associated clay minerals
418 On the basis of a large review of major basin-hosted ore deposits in Europe, Muchez
419 et al. (2005) suspect that most of them formed in extensional settings. Where extension was
420 pronounced and heat production elevated, mineralizing fluids were expelled along extensional
421 faults after having migrated through the sedimentary basin and the basement. This conclusion
422 does not match with the regional illitization episodes in the Les Malines district, which do not
423 occur next to major extensional tectonic or rifting areas. Indeed, the results from southeastern
424 Massif Central confirm the occurrence of two major episodes during the Upper Permian-
425 Lower Triassic and Liassic times far from common tectonic/geodynamic activities, in rather
426 quiescent areas where only re-activation of fault systems could be identified. This lack of
427 physical processes in the neighborhood of the metal deposits needs migrations of hot fluids in
428 the continental crust, as the metals were concentrated at specific places, but not necessarily
429 during all detected tectonic-thermal episodes. Many of such deposits were dated during

Jurassic and Cretaceous episodes at 185 ± 15, 140 ± 10 and 105 ± 5 Ma, which supports a relationship between fluid movements and geodynamic events, however far from major tectonic-thermal events.

In summary, a pre-concentration episode of U was detected at about 270 Ma ago in leucogranite veins. Alternatively, the 250-Ma event identified by K-Ar dating of illite separates obviously did not impact the ores, while the 170 ± 15 Ma episode affected varied types of deposits in the southeastern Massif Central, as well as the 140-Ma and 100-Ma events. Even a more recent event was found at Pierres Plantées at about 35-40 Ma ago. Alternatively, no post 100-Ma event was detected in the clay material, which inclines one to consider that the 35-40 Ma date for coffinite at Pierres Plantées (Respaut et al., 1991) and the more or less associated remagnetization episode at 50-60 Ma at the les Malines (Rouvier et al., 2001) were not generated by thermal events.

Conclusions

Illite-rich size-fractions of Cambrian and Permian calcschists, shales and dolostones of the metallogenic district from southeastern Massif Central were dated by the K-Ar method. The combined mineralogical and K-Ar determinations support the following conclusions:

(1) Illite K-Ar ages suggest crystallization episodes at 288 ± 10, 246 ± 9 and 197 ± 6 Ma. However, all these tectonic-thermal events were not monitored by mineralizing fluids, which seem to have contributed to illitization probably at 136 ± 4 Ma and definitely at 107 ± 4 Ma, evidenced by metal U-Pb and Pb-Pb dating in faults, and during minor Cretaceous pulses.

(2) Fluid events occurred within a segment of a continental margin away from rift zones and from major deformation areas of Western Europe. The lack of important geodynamic activities next to the metal-rich deposits leads the author to consider periodic migration of hot-fluids in the underlying continental crust, as metals were concentrated at specific places, but not necessarily altered by each tectonic-thermal pulse recorded by illite crystallization. The 250-Ma episode, for instance, seems not to have altered the metalliferous concentrations.

(3) The tectonic-thermal history of the Les Malines ore district confirms repetitive geodynamic re-activation of previously occurring events that affected local mass, as well as heat transfer in the plutonic basement and in the overlying sediments. On the other hand, the

461 recent episode at 35-40 Ma ago in coffinite at Pierres Plantées Massif has obviously not been
462 induced by a thermal episode, since it was not recorded in the illite clays.
463
464 ## Acknowledgements
465
466 The K-Ar data discussed in this review come from PhDs of Vella (1989) and Mendez
467 Santizo (1990). They were generated by the isotope team of the Centre de Géochimie de la
468 Surface from Louis Pasteur University of Strasbourg I was heading at the time. They have not
469 been published as such before. I would like to sincerely thank Dr. R. Freeman who reviewed
470 the English presentation, D. Tisserant, Ray. Wendling and R. Winkler the engineers and
471 technician of the isotope team for technical assistance during the K-Ar determinations, as well
472 as J.L. Cezard for the XRD analyses and Rob. Wendling for the clay extractions.
473
474 ## References
475
476 Bell K. (1985) Geochronology of the Carswell area, northern Saskatchewan. In: The Carswell
477 structure uranium deposits, Saskatchewan. Lainé R., Alonso D. and Svab M. (Eds.), Geol.
478 Assoc. of Canada, Spec. Pap., 29, 33-45.
479 Bellon H., Ellenberger F. and Maury R. (1974) Sur le rajeunissement de l'illite des pélites
480 saxoniennes du basin de Lodève. C. R. Acad. Sci. Fr., 278, 413-415.
481 Bernard A.J. (1958) Contribution à l'étude de la province métallifère sous-cévenole. Mém.
482 Sci. Terre, Nancy, 7, 123-403.
483 Bezmen N.I., Tikhomirova V.I. and Kosogova V.P. (1975) Pyrite-pyrrhotite geothermometer:
484 distribution of nickel and cobalt. Geokhimiya, 5, 700-714.
485 Bonhomme M.G., Thuizat R., Pinault Y., Clauer N., Wendling A. and Winkler R. (1975)
486 Méthode de datation Potassium-Argon. Appareillage et technique. Note technique, Inst.
487 Géol., Univ. Strasbourg, 3, 53 pp.
488 Bonhomme M. and Millot G. (1978) Diagenèse généralisée du Jurassique moyen (170-160
489 Ma) dans le basin du Rhône inférieur jusqu'à la bordure des Cévennes (France). C. R.
490 Acad. Sci. Fr., 304, 431-434.
491 Bonhomme M., Bühmann D. and Besnus Y. (1983) Reliability of K-Ar dating of clays and

492 silicifications ssociated with vein mineralizations in Western Europe. Geol. Rdschau, 72,
493 105-117.
494 Bray C.J., Spooner E.T.C., Hall C.M., York D., Bills T.M. and Krueger H.W. (1987) Laser
495 probe $^{40}Ar/^{39}Ar$ and conventional K-Ar dating of illites associated with the McClean
496 unconformity-related uranium deposits, north Saskatchewan, Canada. Can. J. Earth Sci.,
497 24, 10-23.
498 Bril H., Bonhomme M.G., Marcoux E. and Baubron J.C. (1991) Ages K/Ar des
499 minéralisations de Brioude-Massiac (W-Au-As-Sb; Pb-Zn), Pontgibaud (Pb-Ag; Sn), et
500 Labessette (As-Pb-Sb-Au): Place de ces districts dans l'évolution géotectonique du Massif
501 central français. Min. Depos., 26, 189-198.
502 Brockamp O., Zuther M. and Clauer N. (1987) Epigenetic-hydrothermal origin of the
503 sediment-hosted Muellenbach uranium deposit, Baden-Baden, W-Germany. Monogr. Ser.
504 on Min. Depos., 27, 87-98.
505 Brockamp O. and Clauer N. (2013) Hydrothermal and unexpected diagenetic alteration in
506 Permian shales of the Lodève epigenetic U-deposit of southern France, traced by K-Ar
507 illite and K-feldspar dating. Chem. Geol. 357, 18-28.
508 Cathelineau M., Fourcade S., Clauer N., Buschaert S., Rousset D., Boiron M.C., Meunier A.,
509 Lavastre V. and Javoy M. (2004) Dating multistage paleofluid percolations: A K-Ar and
510 ^{18}O study of fracture illites from altered Hercynian plutonites at the basement/cover
511 interface (Poitou High, France). Geochim. Cosmochim. Acta, 68, 2529-2542.
512 Cathelineau M., Boiron M.C., Fourcade S., Ruffet G., Clauer N., Belcourt O., Coulibaly Y.,
513 Banks D.A. and Guillocheau F. (2012) A major Late Jurassic fluid event at the
514 basin/basement unconformity in western France: $^{40}Ar/^{39}Ar$ and K-Ar dating, fluid
515 chemistry, and related geodynamic context. Chem. Geol., 322-323, 99-120.
516 Charef A. and Sheppard S.M.F. (1988) The Malines Cambrian carbonate-shale-hosted Pb-Zn
517 deposit, France: Thermometric and isotopic (H, O) evidence for pulsating hydrothermal
518 mineralization. Miner. Depos., 23, 86-95.
519 Clauer N., Ey F. and Gauthier-Lafaye F. (1985) K-Ar dating of different rock types from the
520 Cluff Lake uranium ore deposits (Saskatchewan-Canada). In: The Carswell structure
521 uranium deposits, Saskatchewan. Lainé R., Alonso D. and Svab M. (Eds), Spec. Pap.,
522 Geol. Assoc. Canada, 29, 47-53.

523 Clauer N. and Chaudhuri S. (1992) Indirect dating of sediment-hosted ore deposits: Promises
524 and problems. In: Isotopic signatures and Sedimentary Records. Clauer N. and Chaudhuri
525 S. (Eds.), Lect. Not. in Earth Sci., Springer Verlag, Heidelberg, 43, 361-388.
526 Clauer N. and Chaudhuri S. (1995) Clays in crustal environments. Isotope dating and tracing.
527 Springer Verlag, Heidelberg, 359 p.
528 Clauer N., Weber F., Gauthier-Lafaye F., Toulkeridis T. and Sizun J.P. (1997) Mineralogical,
529 geochemical (REE), and isotopic (K-Ar, Rb-Sr, $\delta^{18}O$) evolution of the clay minerals from
530 faulted, carbonate-rich, passive paleomargin of Southeastern Massif Central, France. J.
531 Sedim. Res., 67, 923-934.
532 Clauer N. and Chaudhuri S. (1998) Isotopic dating of very low-grade metasedimentary and
533 metavolcanic rocks: techniques and methods. In: Low-Grade Metamorphism. Frey M. and
534 Robinson D. (Eds.), Blackwell Science, Oxford, 202-226.
535 Clauer N., Zwingmann H., Liewig N. and Wendling R. (2012) Comparative $^{40}Ar/^{39}Ar$ and K-
536 Ar dating of illite-type clay minerals: A tentative explanation for the age identities and
537 differences. Earth Sci. Rev., 115, 76-96.
538 Clauer N. (2013) The K-Ar and $^{40}Ar/^{39}Ar$ methods revisited for dating fine-grained K-bearing
539 clay minerals. Chem. Geol., 354, 163-185.
540 Connan J. and Orgeval J.J. (1977) Un exemple d'application de la géochimie organique en
541 métallogénie : la mine des Malines (Gard, France). Bull. Cent. Rech. Expl. Prod. Elf
542 Aquitaine, 1, 59-105.
543 Dromart G., Allemand P. and Quiquerez A. (1998) Calculating rates of syndepositional
544 normal faulting in the western margin of the Mesozoic Subalpine Basin (south-east
545 France). Bas. Res., 10, 235–260.
546 Fogliérini F., Bernard A. and Verraes G. (1980) Le gisement Zn-Pb des Malines (Gard).
547 Gisement Français, Fasc. E5 26e CGI, Dél. Gén. Rech. Scien. Techn., 56 p.
548 Halliday A.N. and Mitchell J.G. (1983) K-Ar ages of clay concentrates from Irish ore-bodies
549 and their bearing on the timing of mineralization. Trans. Roy. Soc. Edinburgh Earth Sci.,
550 74, 1-14.
551 Halter G., Sheppard S.M.F., Weber F., Clauer N. and Pagel M. (1987) Radiation-related
552 retrograde hydrogen isotope and K-Ar exchange in clay minerals. Nature, 330, 638-641.

553 Hamet J. and Mattauer M. (1977) Age hercynien déterminé par la méthode ^{87}Rb-^{87}Sr du
554 granite de l'Aigoual. Conséquences structurales. C. R. Somm. Soc. Géol. Fr., 2, 80-84.
555 Harper C.T. (1970) Graphic solution to the problem of ^{40}Ar loss from metamorphic minerals.
556 Eclog. Geol. Helv., 63, 119-140.
557 Henry B., Rouvier H., Le Goff M., Leach D., Macquar J.-C., Thibieroz J. and Lewchuk M.T.
558 (2001) Palaeomagnetic dating of widespread remagnetization on the southeastern border of
559 the French Massif Central and implications for fluid flow and Mississippi Valley-type
560 mineralization. Geophys. Jour. Intern., 145, 368-380,
561 Holliger P., Pagel M. and Pironon J. (1989) A model for ^{238}U radioactive daughter loss
562 from sediment-hosted pitchblende deposits and the Late Permian-Early Triassic
563 depositional U-Pb age of the Müllenbach uranium ore (Baden-Württemberg, F.R.G.)
564 Chem. Geol. (Isot. Geosci. Sect.), 80, 45–53.
565 Ineson P.R., Mitchell J.C. and Vokes F.M. (1975) K-Ar dating of epigenetic mineral deposits:
566 An investigation of the Permian metallogenic province of the Oslo region, Southern
567 Norway. Econ. Geol., 70, 1426-1436.
568 Kotzer T.G. and Kyser T.K. (1995) Petrogenesis of the Proterozoic Athabasca Basin,
569 Northern Saskatchewan, Canada, and its relation to diagenesis, hydrothermal uranium
570 mineralization paleohydrogeology. Chem. Geol., 120, 45-89.
571 Kübler B. (1968) Evaluation quantitative du métamorphisme par la cristallinité de l'illite.
572 Bull. Cent. Rech. de Pau, SNPA, 285-397.
573 Kübler B. (1997) Concomitant alteration of clay minerals and organic matter during burial
574 diagenesis. In: Soils and sediments. Paquet H. and Clauer N. (Eds.), Springer Verlag, 327-
575 362.
576 Kyser K., Hiatt E., Renac C., Durocher K., Holk G. and Deckart K. (2000) Diagenetic fluids
577 in paleo- and meso-Proterozoic sedimentary basins and their implications for long
578 protracted fluid histories. In: Fluids and Basin Evolution. Kyser K. (Ed.). Miner. Assoc.
579 Canada, Short Course Series, 28, 225-262.
580 Lancelot J. and Vella V. (1989) Datation U-Pb liasique de la pechblende de Rabejac. Mise en
581 évidence d'une préconcentration uranifère permienne dans le basin de Lodève (Hérault).
582 Bull. Soc. Géol.. Fr., 8, 309-315.

583 Lancelot J.R., de Saint André B. and de la Boisse H. (1994) Systématique U-Pb et évolution
584 du gisement d'uranium de Lodève (France). Mineral. Depos., 19, 44-53.
585 Lancelot J., Briqueu L., Respaut J.P. and Clauer N. (1995) Géochimie isotopique des
586 systèmes U-Pb/Pb-Pb et évolution polyphasée des gîtes d'uranium du Lodévois et du sud
587 du Massif Central. Chron. Rech. Min., 521, 3-18.
588 Laverret E., Clauer N., Fallick A., Patrier P., Beaufort D., Quirt D., Kister P. and Bruneton P.
589 (2010) K-Ar, $\delta^{18}O$ and δD tracing of illitization within and outside the Shea Creek uranium
590 prospect, Athabasca Basin, Canada. Appl. Geochem., 25, 856-871.
591 Leach D.L., Bradley D., Lewchuk M.T., Symons D.T.A., De Marsily G. and Brannon J.
592 (2001) Mississippi Valley-type lead-zinc deposits through geological time: implications
593 from recent age-dating research. Mineral. Depos., 36, 711-740.
594 Lee M.J. and Brookins D.G. (1978) Rubidium-strontium minimum ages of sedimentation,
595 uranium mineralization, and provenance, Morrison Formation (Upper Jurassic), Grants
596 mineral belt, New Mexico. Amer. Assoc. Petrol. Geol. Bull., 62, 1673-1683.
597 Le Guen M. and Combes P.J. (1988) Typologie des minéralisations plombo-zincifères
598 associées au Bathonien des Malines (Gard, France). Doc. Bur. Rec. Géol. Min., 135, 821-
599 841.
600 Le Guen M., Orgeval J.-J. and Lancelot J. (1991) Lead isotope behaviour in a polyphased Pb-
601 Zn ore deposit, Les Malines (Cévennes, France). Miner. Depos., 26, 150-188.
602 Lemoine M. (1984) La marge occidentale de la Téthys Ligure et les Alpes occidentales. In :
603 Les marges continentales actuelles et fossiles autour de la France, Boillot G., Montadert L.,
604 Lemoine M. et Biju-Duval B. (Eds.), Masson, Paris, 125-248.
605 Lemoine M., Bas T., Arnaud-Vanneau A., Arnaud H., Dumont T., Gidon M., Bourbon M., de
606 Graciansky P.C., Rudkiewicz J.L., Megard-Galli J. and Tricart P. (1986) The continental
607 margin of the Mesozoic Tethys in the Western Alps. Mar. Petrol. Geol., 3, 179–199.
608 Léveque M.H., Lancelot J. and George E. (1988) The Bertholène uranium ore deposit:
609 mineralogical characteristics and U-Pb dating of a primary U mineralization and its
610 subsequent remobilization. Consequences upon the evolution of the U ore deposits of the
611 Massif Central. Chem. Geol., 69, 147-163.
612 Liewig N., Clauer N. and Sommer F. (1987) Rb-Sr and K–Ar dating of clay diagenesis in
613 Jurassic sandstone reservoirs. Amer. Assoc. Petrol. Geol. Bull. 71, 1467-1474.

614 Macquar J.C. (1970) Le Trias. Bull. Bur. Rech. Géol. Min., 2, II 1, 27-65.
615 Macquar J.-C., Rouvier H. and Thibiéroz J. (1990) Les minéralisations Zn, Pb, Fe, Ba, F péri-
616 cévenoles: cadre structuro-sédimentaire et distribution spatio-temporelle. In: Mobilité et
617 concentration des métaux de base dans les couvertures sédimentaires, Manifestations,
618 Mécanismes, Prospections. Pélissonier H., Sureau J.F. (Eds.), Doc. BRGM, 158, 143-158.
619 Mendez Santizo J. (1990) Diagenèse et circulations de fluids dans le gisement d'uranium de
620 Lodève (Hérault). PhD Thesis, Strabourg University, 166p.
621 Mendez Santizo J., Gauthier-Lafaye F., Liewig N., Clauer N. and Weber F. (1991) Existence
622 d'un hydrothermalisme tardif dans le bassin de Lodève (Hérault). Arguments
623 paléothermométriques et géochronologiques. C. R. Acad. Sci., Paris, 312, 739-745.
624 Merignac C. and Cuney M. (1999) Ore deposits of the French Massif central: Insight into the
625 metallogenesis of the Variscan collision belt. Miner. Depos., 34, 472-504.
626 Michaud J.G. (1970) Gisements de Pb-Zn du Sud du Massif Central français (Cévennes-
627 Montagne Noire) et caractéristiques géologiques de leur environnement. Bull. Cent. Rech.
628 Expl. Prod. Elf Aquitaine, 3, 335-380.
629 Miller D.S. and Kulp J.L. (1963) Isotopic Evidence on the origin of the Colorado Plateau
630 Uranium ores. Geol. Soc. Amer. Bull., 75, 609-630.
631 Montadert L., Roberts D.G., de Charpal O. and Guennoc P. (1979) Rifting and subsidence of
632 the northern continental margin of the Bay of Biscaye. In: Montadert L., Roberts D.G. et
633 al. (Eds.), Init. Rep. Deep Sea Drill. Proj., 48. U.S. Govern. Print. Office, Washington,
634 1025–1060.
635 Muchez P., Heijlen W., Banks D., Blundell D., Boni M. and Grandia F. (2005) Extensional
636 tectonics and the timing and formation of basin-hosted deposits in Europe. Ore Geol. Rev.,
637 27, 241-267.
638 Nier A.O. (1950) A redetermination of the relative abundances of the isotopes of carbon,
639 nitrogen, oxygen, argon and potassium. Phys. Rev., 77, 789-793
640 Odin G.S. and 35 collaborators (1982) Interlaboratory standards for dating purposes. In:
641 Numerical dating in Stratigraphy, Odin G.S. (Ed.), J. Wiley & Sons Ltd, 123-158.
642 Orgeval J.J. (1976) Les remplissages karstiques minéralisés : exemple de la mine des Malines
643 (Gard, France). Mém. H. Sér. Soc. Géol. Fr., 7, 77-85.

644 Polito P.A., Kyser T.K. and Jackson M.J. (2006) The role of sandstone diagenesis and aquifer
645 evolution in the formation of uranium and zinc-lead deposits, southern McArthur Basin,
646 Northern Territory, Australia. Econ. Geol., 101, 1189-1209.
647 Ramboz C.C. (1989) Conditions of fluid circulation in rifts : comparison between the
648 Subalpine Basin and the Central Red Sea. E.U.G., Strasbourg, Terra Cognita Abstracts, 1,
649 p. 202.
650 Respaut J.P., Cathelineau M. and Lancelot J. (1991) Multistage evolution of the Pierres
651 Plantées uranium ore deposit (Margeride, France): evidence from mineralogy and U-Pb
652 systematics. Eur. J. Min., 3, 85-103.
653 Romer R.L. (2001) Lead incorporation during crystal growth and the misinterpretation of
654 geochronological data from low $^{238}U/^{204}Pb$ metamorphic minerals. Terra Nova, 13, 258-
655 263.
656 Rouvier H., Henry B., Macquar J.C., Leach D, Le Goff M., Thieberoz J. and Lewchuk T.
657 (2001) Réaimantation régionale éocène, migration de fluides et minéralisations sur la
658 bordure cévenole (France). Bull. Soc. Géol. France, 172, 503– 16.
659 Santouil G. (1980) Tectonique et microtectonique comparée de la distension permienne et de
660 l'évolution post-triasique dans les bassins de Lodève, Saint-Affrique et Rodez (France SE).
661 Master Thesis, Montpellier University , 62 p.
662 Staffelbach C., Mendez Santizo J., Horrenberger J.C., Ruhland M. and Weber F. (1987)
663 Metallogenesis of uranium deposits. AIEA Proceed. Techn. Commit. Meet., Vienna 9-
664 12/03/87, 119-135.
665 Steiger R. H. and Jäger E. (1977) Subcommission on geochronology: convention on the use of
666 decay constants in geo- and cosmochronology. Earth Plan. Sci. Lett., 36, 359-362.
667 Turpin L., Clauer N., Forbes P. and Pagel M. (1991) U-Pb, Sm-Nd and K-Ar systematics of
668 the Akouta uranium deposit, Niger. Chem. Geol., Isot. Geosc. Sect., 87, 217-230.
669 Velde B. (1985) Clay Minerals: a physico-chemical explanation of their occurrence. Develop
670 in Sedim., Elsevier, Amsterdam, 40, 426 p.
671 Vella V. (1989) Les chronomètres U-Pb, Rb-Sr, K-Ar appliqués à l'évolution d'un gisement
672 uranifère en milieu sédimentaire; Cas du Bassin de Lodève (Hérault). PhD Thesis,
673 Montpellier University, 133p.

674 Verraes G. (1983) Etude monographique du district minier des Malines et de ses environs
675 (province sous cévenole, France). PhD Thesis, University Montpellier, 591p.
676 Vialette Y. and Sabourdy G. (1977) Age du granite de l'Aigoual dans le massif des Cévennes
677 (France). C. R. Somm. Soc. Géol. France, 3, 130-132.
678 Wilson M.R., Kyser T.K., Mehnert H.H. and Hoeve J. (1987) Changes in the H-O-Ar isotope
679 composition of clays during retrograde alteration. Geochim. Cosmochim. Acta, 51, 869-
680 878.

681

682

683 Figure and table captions

684

685 **Figure 1:** (A) Geographic distribution of the samples from French Massif Central studied
686 here and earlier (modified from Merignac and Cuney, 1999, and from Santouil, 1980). (B)
687 Details of the Montdardier - Les Malines district with the locations of the sampling sites;
688 (C) Details of the Lodève district with the locations of the sampling sites (modified from
689 Santouil, 1980, where the rock types are identified).

690

691 **Figure 2:** Radiogenic ^{40}Ar vs. K_2O histogram (Harper, 1970) of the different illite-rich size
692 fractions and the feldspar separates of this study.

693

694 **Figure 3:** Synthetic sketch of the regional K-Ar illite ages and U-Pb and Pb-Pb ages of metal-
695 rich deposits from French Massif Central. The locations are in the figure 1A. The origins
696 of the results are given below the diagram. The thick age-sector arrows were obtained on
697 variable illite size fractions, while the thin sector arrows were obtained on <2 μm illite size
698 fractions.

699

700

701 **Table 1:** Location, stratigraphic position and description of the studied samples.

702

703 **Table 2:** XRD mineralogical data of the studied size fractions.

704

705 **Table 3:** K-Ar results of the studied illite-rich size fractions and feldspar separates. Ar*
706 stands for radiogenic Ar.

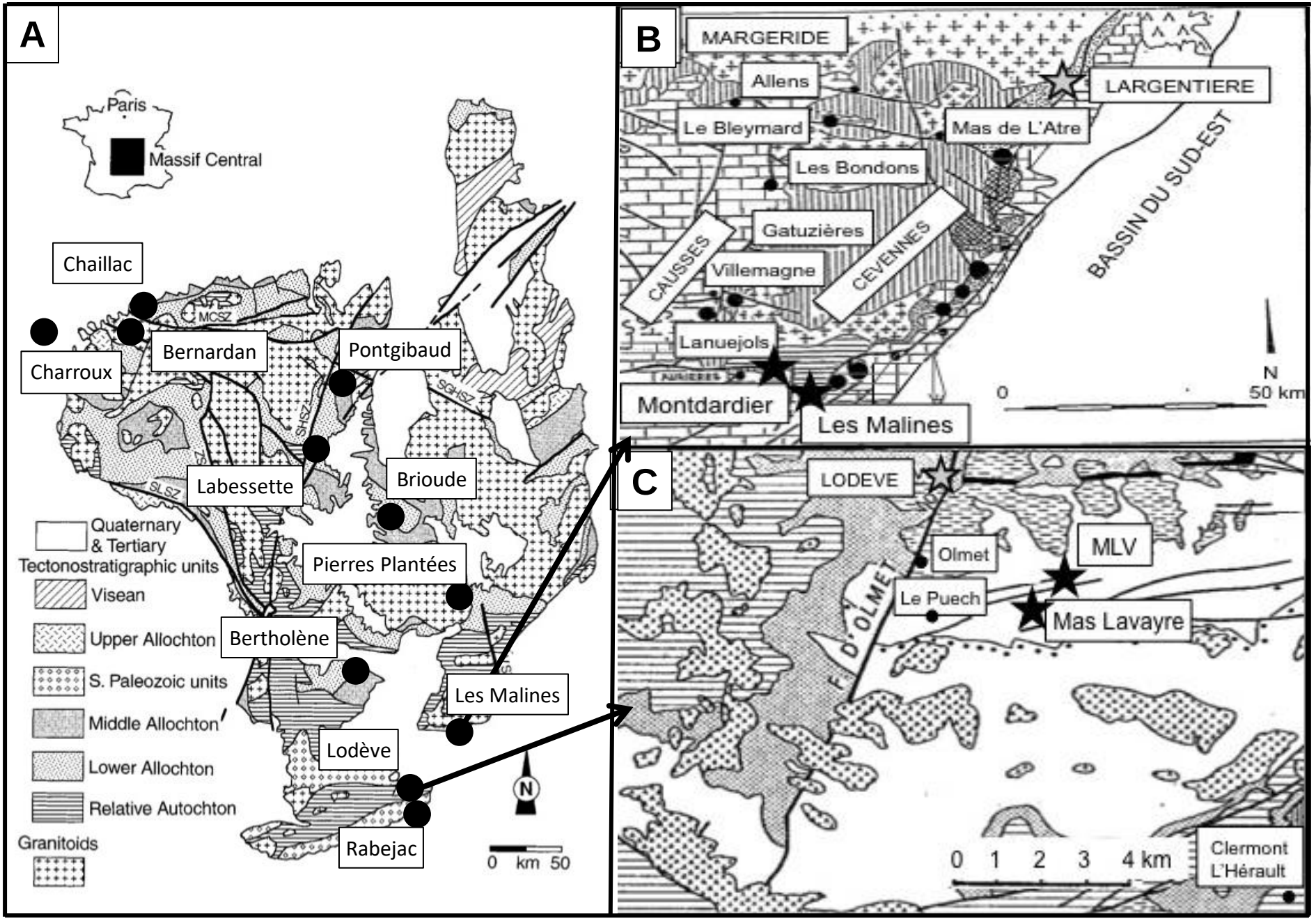
A
Paris
Massif Central
Chaillac
Charroux
Bernardan
Pontgibaud
Labessette
Brioude
Pierres Plantées
Bertholène
Les Malines
Lodève
Rabejac
MCSZ
SHSZ
SGHSZ
SLSZ
Quaternary & Tertiary
Tectonostratigraphic units
Visean
Upper Allochton
S. Paleozoic units
Middle Allochton
Lower Allochton
Relative Autochton
Granitoids
N
0 km 50
B
MARGERIDE
Allens
LARGENTIERE
Le Bleymard
Mas de L'Atre
Les Bondons
Gatuzières
CAUSSES
CEVENNES
BASSIN DU SUD-EST
Villemagne
Lanuejols
Montdardier
Les Malines
N
0
50 km
C
LODEVE
Olmet
MLV
Le Puech
Mas Lavayre
F. D'OLMET
0 1 2 3 4 km
Clermont L'Hérault

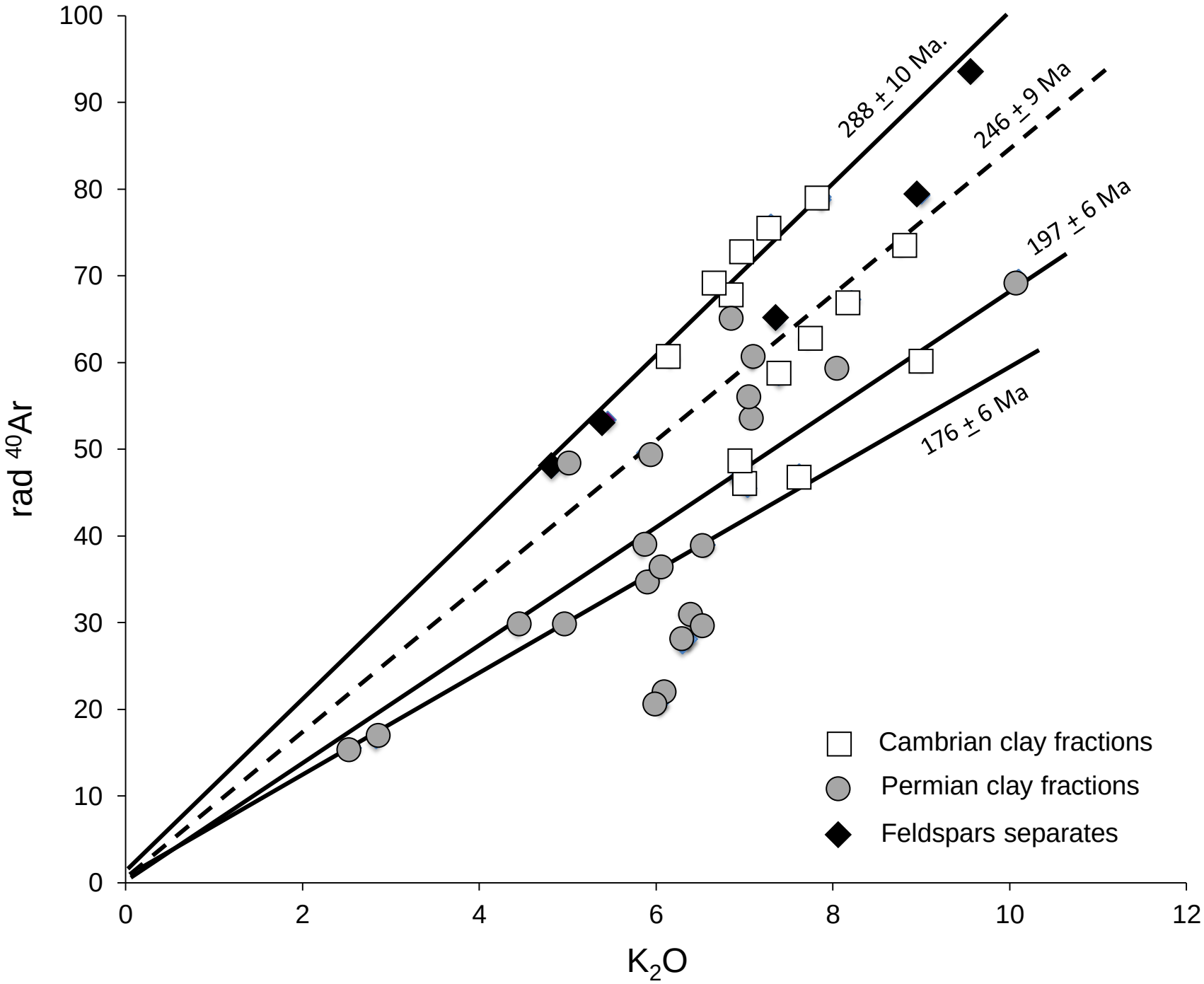
100
90
80
70
60
50
40
30
20
10
0
0
2
4
6
8
10
12
rad ^{40}Ar
K_2O
288 ± 10 Ma.
246 ± 9 Ma
197 ± 6 Ma
176 ± 6 Ma
Cambrian clay fractions
Permian clay fractions
Feldspars separates

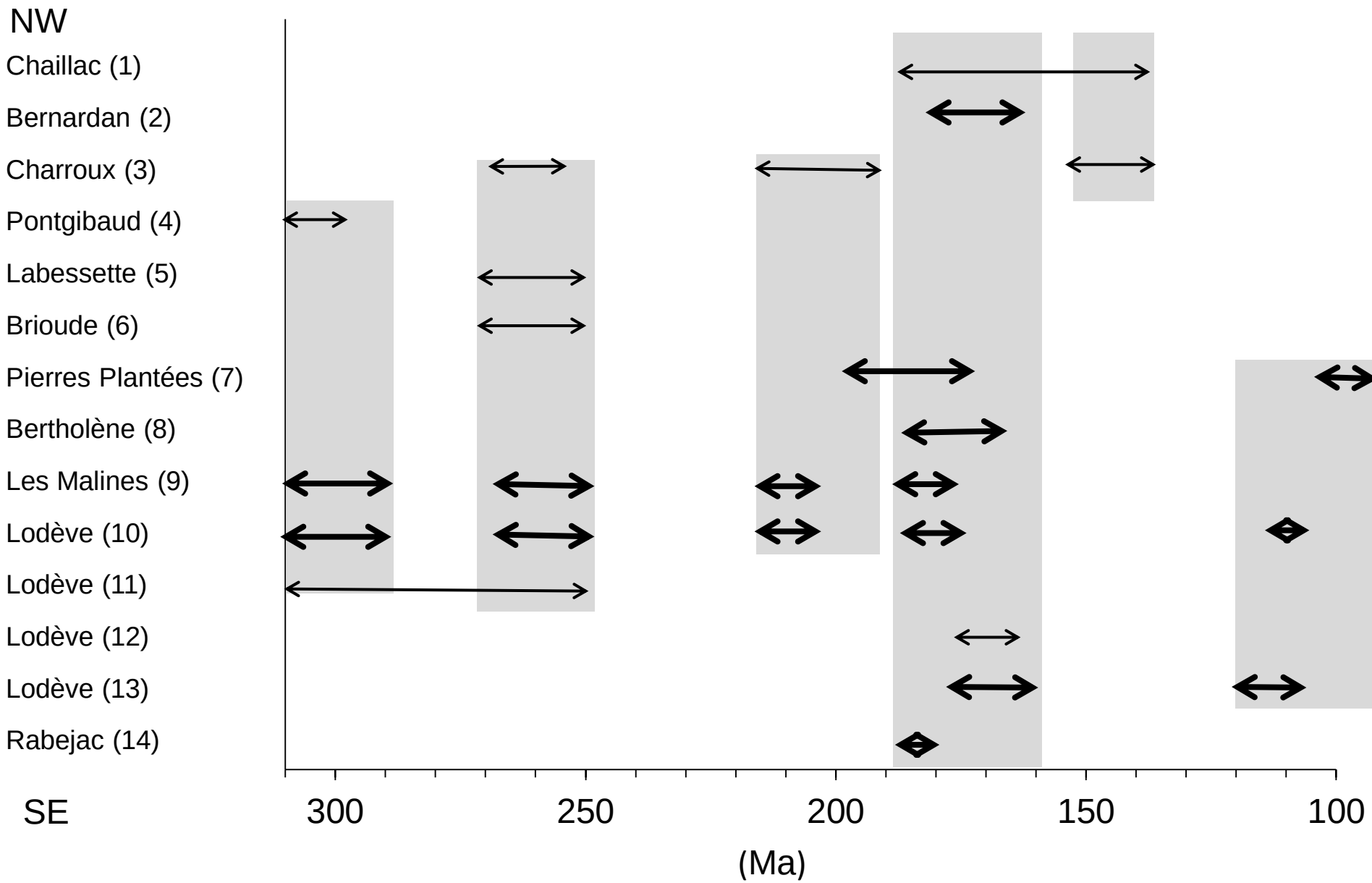

Data (1) and (3) of Cathelineau et al. (2004; 2012); data (2) of Clauer (unpublished); data (4, 5 and 6) of Bril et al. (1991); data (7) of Respaut et al. (1991); data (8) of Schmitt et al. (1984) and Lévèque et al. (1988); data (9 and 10) of this review; data (11) of Brockamp and Clauer (2013); data (12) of Bellon et al. (1974); data (13 and 14) of Lancelot and Vella (1989).

Sample ID	Stratigraphy	Sample description
Montdardier Mt1	Cambrian	Mine, eastern wall, argillaceous dolomite
Montdardier Mt2		Mine, northern wall, calcschist sampled 1 m below a pyrite layer
Montdardier Mt3		Mine, the same unit at the contact with the pyrite layer
Montdardier Mt4		Mine, the same location, pyrite layer
Montdardier Mt5		Mine, the same location, breccia at the top of the pyrite layer
Montdardier Mt6		Mine, sampled 1 m above in the same facies
Montdardier MS1		Mine, excavation surface close to an important ore concentration
Montdardier F1		Core, mineralized sample from F18 drilling into an excavation
Montdardier F2		Core, sample from F19 drilling to the N of Montardier mine
Les Malines LM1		Mine, argillaceous dolomite with sphalerite in veinlets
Les Malines LM2		Mine, argillaceous dolomite in a cavity of dolostones
Mas Lavayre ML1	Permian	Mine, greyish silt with some bituminous inclusions
Mas Lavayre ML2		Mine, grey-to-red sandy shale
Mas Lavayre ML3		Mine, redish pelite with bituminous stratiform accumulations
Mas Lavayre ML4		Mine, redish pelite
Mas Lavayre SJ2		Mine, eastern wall Saint Julien fault, 4 m away from main fault
Mas Lavayre SJ3		Mine, eastern wall, Saint Julien fault, 1 m from a lateral fault
Mas Lavayre SJ4		Mine, eastern Saint Julien fault, within a lateral fault
Mas Lavayre SJ5		Mine, eastern wall, Saint Julien fault, 0.5 m off the lateral fault
Mas Lavayre SJ6		Mine, eastern Saint Julien fault, 5 m from lateral fault
MVL354 (93m) MVL1		Drilling core, barren shale
MLV354 (94m) MLV2		Drilling core, barren shale on top of a bituminous dolomitic shale
MLV354 (236m) MLV3		Drilling core, sandy pelite
MLV354 (286m) MLV4		Drilling core, dolomitic shale above an uraniferous bitumen concentration
MLV354 (286.5m) MLV5		Drilling core, bituminous shale
MLV354 (287m) MLV6		Drilling core; shale with uranium concentrates

Sample ID	Stratigraphy	Size (μm)	Illite (%)	I-S (%)	Kaolinite (%)	Chlorite (%)	Acc.	FWHM
Montdardier M1	Cambrian	<0.4	100		tr		-	0.50
		0.4-2	85		15		Q, F	0.29
Montdardier M2		<2	100				Q, F	0.23
Montdardier M3		<2	90		10		Q, F	0.27
Montdardier M4		<2	100				Q	0.36
Montdardier M5		<0.4	100				-	0.35
		0.4-2	100				Q, F	0.21
Montdardier M6		<2	100				Q, F	0.29
Montdardier DS1		<2	100				-	n.d.
Montdardier F1		<2	100				Q	n.d.
Montdardier F2		<2	100				-	n.d.
Les Malines LM1		<2	100				q	0.28
Les Malines LM2		<2	100				q, F	0.30
Mas Lavayre ML1	Permian	<2	25	15		60	f	n.d.
Mas Lavayre ML2		<2	55			45	Q, f	n.d.
Mas Lavayre ML3		<2	35			65	Q, F	n.d.
Mas Lavayre ML4		<2	40	15		45	F	n.d.
Mas Lavayre SJ2*		<0.4	0	70		30	-	n.d.
Mas Lavayre SJ3*		<0.4	60	10		30	-	n.d.
Mas Lavayre SJ4*		<0.4	35	50		15	-	n.d.
Mas Lavayre SJ5*		<0.4	70			30	-	0.52
Mas Lavayre SJ6*		<0.4	60			40	-	n.d.
MLV354 (93m) MLV1		<2	80			20	f	0.45
MLV354 (94m) MLV2		<2	80			20	F	0.45
MLV354 (236m) MLV3		<2	20			80	Q, F	n.d.
MLV354 (286m) MLV4		<2	10			90	F	n.d.
MLV354 (286.5m) MLV5		<2	10			90	f, q	n.d.
MLV354(287m) MLV6		<2	0	15		85	f	n.d.

I-S stands for illite-smectite mixed layer, F for feldspar, Q for quartz, both in small lettering when in trace amounts, n.d. f not determined ; Acc. for accessory minerals and FWHM for Full Width at Half Maximum

Sample ID	Stratigraphy	Sizes (μm)	K_2O (%)	Ar* (%)	40Ar* (10-6 cm3/g)	K-Ar ages (Ma ± 2σ)
Clay fractions						
Montdarier M1	Cambrian	<0.4	9.01	95.81	60.27	196.5 (4.2)
		0.4-2	8.21	96.65	67.32	238.0 (5.1)
Montdardier M2		<2	7.72	88.17	62.89	236.6 (6.6)
Montdardier M3		<2	7.87	66.25	78.79	286.7 (9.8)
Montdardier M4		<2	6.81	45.57	67.68	284.7 (13.3)
Montdardier M5		<0.4	8.77	94.90	73.59	243.2 (5.3)
		0.4-2	7.30	96.80	76.09	297.5 (6.4)
Montdardier M6		<2	6.97	46.40	72.85	298.3 (13.7)
Montdardier DS1		<2	7.62	92.40	47.31	183.0 (4.1)
Montdardier F1		<2	7.01	87.80	48.44	202.6 (4.8)
Montdardier F2		<2	7.03	89.30	45.55	190.6 (4.4)
Les Malines LM1		<0.4	6.16	54.74	60.72	282.6 (10.5)
		0.4-2	6.66	84.74	69.05	296.1 (7.3)
Les Mlines LM2		<0.4	7.39	54.92	58.40	229.9 (8.5)
Mas Lavayre ML1	Permian	<0.4	6.30	79.20	27.46	130.4 (3.9)
		0.4-2	6.05	90.50	36.35	177.4 (4.1)
		<2	5.89	71.60	30.67	154.8 (4.5)
Mas Lavayre ML2		<2	8.06	66.50	59.56	215.8 (6.6)
Mas Lavayre ML3		<2	4.43	46.70	29.62	196.4 (8.6)
Mas Lavayre ML4		<2	10.10	91.20	69.71	202.4 (4.5)
Mas Lavayre SJ2		<0.4	6.50	75.92	29.71	136.5 (3.7)
		0.4-1	6.56	86.45	38.96	175.5 (4.2)
Mas Lavayre SJ3		<0.2	6.36	71.65	28.07	132.0 (4.3)
		<0.4	6.43	78.07	30.24	140.3 (3.7)
		0.4-1	5.93	78.06	35.17	175.3 ('.7)
Mas Lavayre SJ4		<0.2	6.04	58.84	20.67	103.0 (3.5)
		<0.4	6.10	76.97	22.31	110.1 (3.0)
		0.4-1	6.36	76.93	31.23	146.3 (3.9)
Mas Lavayre SJ5		<0.4	6.93	85.73	46.80	198.3 (4.8)
		0.4-1	7.05	86.65	53.85	222.7 (5.3)
Mas Lavayre SJ6		<0.2	7.05	85.99	55.95	230.8 (6.5)
		<0.4	7.09	90.15	60.53	247.2 (5.7)
		0.4-1	6.85	89.70	65.92	276.3 (6.9)
MLV354 (93m) MLV1		<2	5.81	91.10	48.22	240.8 (5.5)
MLV354 (94m) MLV2		<0.4	5.88	66.50	49.53	244.1 (8.3)
		0.4-2	4.98	75.50	48.20	277.8 (7.8)
MVL354 (236m) MLV3		<0.4	4.95	42.70	30.00	178.9 (8.7)
		0.4-2	5.84	54.30	38.81	195.2 (7.3)
MLV354 (286m) MLV4		<0.4	2.83	69.90	16.57	173.1 (7.5)
		0.4-2	2.56	85.40	15.53	179.1 (4.8)
MLV354 (286m) MLV5		<2	2.56	80.60	15.98	184.1 (5.0)
MLV354 (287m) MLV6		<2	4.11	84.70	23.56	169.7 (4.3)
Feldspar separates						
Mas Lavayre F1a		80-100	4.82	45.22	47.71	283.6 (13.0)
Mas Lavayre F1b		100-125	5.45	52.43	53.38	280.9 (11.6)
Mas Lavayre F1c		125-200	9.00	76.90	79.29	254.5 (7.5)
Mas Lavayre F1d		200-400	7.36	62.18	64.82	254.5 (8.9)
Mas Lavayre F2		125-200	9.56	85.32	93.67	281.0 (7.6)

Ar* stands for radiogenic Ar, and SJ for Saint-Julien fault

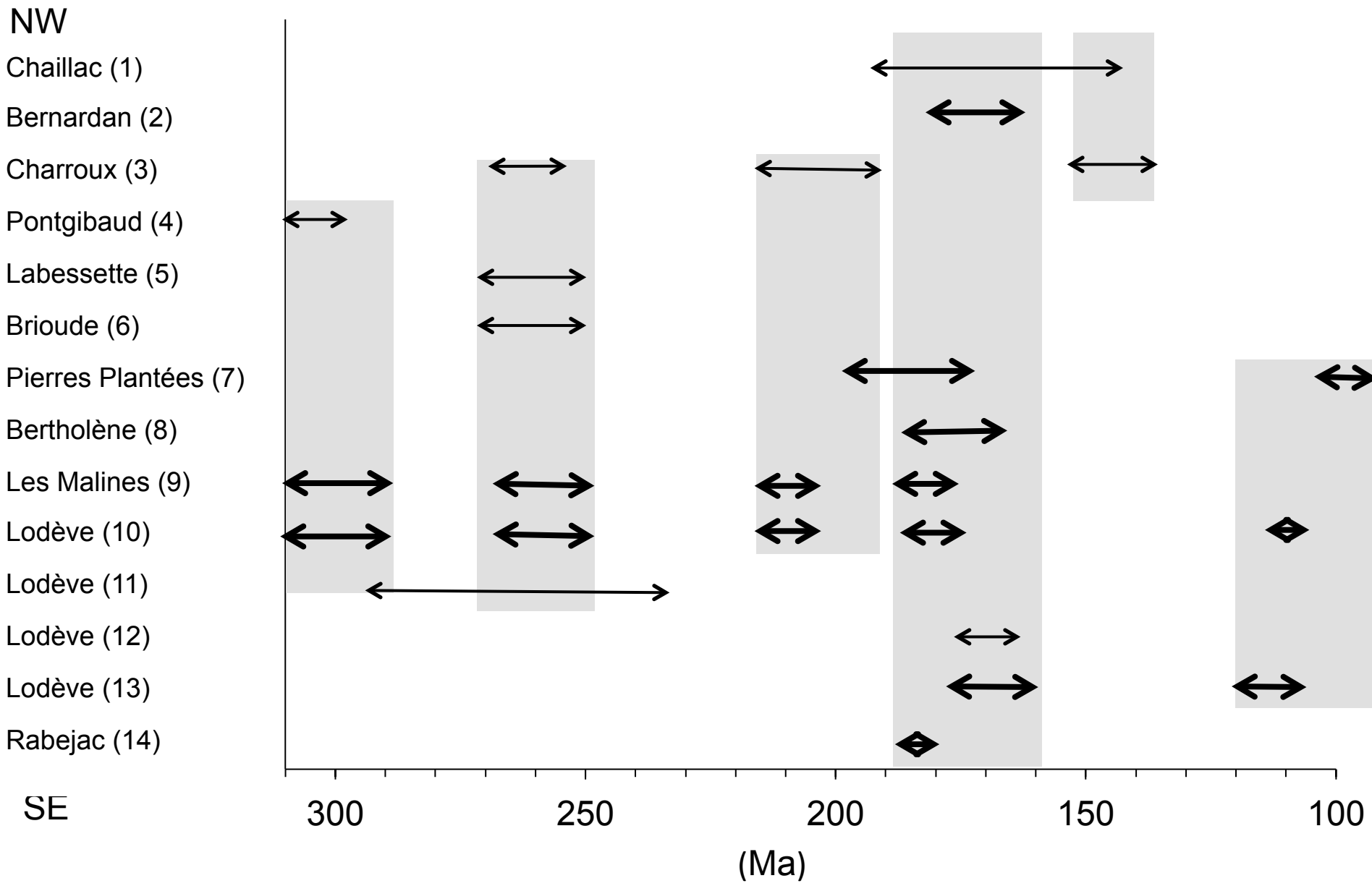

Data (1) and (3) of Cathelineau et al. (2004; 2012); data (2) of Clauer (unpublished); data (4, 5 and 6) of Bril et al. (1991); data (7) of Respaut et al. (1991); data (8) of Schmitt et al. (1984) and Lévèque et al. (1988); data (9 and 10) of this review; data (11) of Brockamp and Clauer (2013); data (12) of Bellon et al. (1974); data (13 and 14) of Lancelot and Vella (1989).